

Y.-W. Lui, H.L. Clark and D.H. Youngblood

Recent studies of the isoscalar giant monopole resonance (GMR) in  $^{40}\text{Ca}$  [1],  $^{28}\text{Si}$  [2] and  $^{24}\text{Mg}$  [3] showed that more than 50% of the E0 energy weighted sum rule (EWSR) were identified. These results are different to the earlier report on the GMR in  $^{58}\text{Ni}$  which located only 32% of the E0 EWSR [4]. With a large fraction of strength missing, the centroid of the GMR cannot be determined reliably and it can distort the overall picture of the GMR systematics.

The long focal plane detector used in  $^{40}\text{Ca}$ ,  $^{28}\text{Si}$  and  $^{24}\text{Mg}$  was clearly necessary in determining both the overall shape as well as the amplitude of the continuum since a significant amount of E0 EWSR was located at higher excitation region ( $>28$  MeV). This detector was not available in the earlier measurement of  $^{58}\text{Ni}$  and it could be necessary to find out the missing strength. Therefore we have remeasured the GMR strength distribution in  $^{58}\text{Ni}$ .

A 240 MeV  $\alpha$  beam from the Texas A&M K500 super-conducting cyclotron was used to bombard a  $4.02\text{ mg/cm}^2$   $^{58}\text{Ni}$  metal foil located in the target chamber of the multipole-dipole-multipole (MDM) spectrometer. Inelastically scattered  $\alpha$  particles were detected in the focal plane detector which covered approximately 55 MeV of excitation from 7 MeV  $<E_x < 62$  MeV and measured position and the angle in the scattering plane. The out-of-plane scattering angle,  $\phi$  was not measured. Position resolution of approximately 0.9 mm and the scattering angle resolution of about  $0.09^\circ$  were obtained. The experimental technique has been described in details in Ref. [1] and [2].

Data were taken with the spectrometer at  $0.0^\circ$  ( $0.0^\circ < \Theta < 2.0^\circ$ ) and at  $3.5^\circ$  ( $1.5^\circ < \Theta < 5.5^\circ$ ). Each data set was divided into ten angle bins, each corresponding to  $\delta\Theta \approx 0.4^\circ$  using the angle obtained from ray tracing.  $\phi$  is not measured by the detector, so the average angle for each bin was obtained by integrating over the height of the solid angle defining slit and the width of the angle bin. Cross-sections were obtained from the charge collected, target thickness, dead time and known solid angle, etc. result in about a  $\pm 10\%$  uncertainty in absolute cross sections. The cross-sections obtained agreed within the error with earlier data [4].

Analyses of the GMR were performed with two different methods, spectrum subtraction and slice analysis. From the results of the light nuclei and from  $^{90}\text{Zr}$  [5], the shape of the E0 strength distribution is not necessary Gaussian, therefore the Gaussian peak fitting analysis reported for the earlier  $^{58}\text{Ni}$  data was not used in this data analysis. The details of the analysis techniques were described in Refs. [2] and [3].

#### Spectrum Subtraction Method

Figure 1a.,b. show raw spectra obtained for two angles and the subtracted spectrum ( $1.1^\circ$ - $1.8^\circ$ ) is shown in Fig. 1c. The broad peak located between 12.00 to 26.00 MeV in the subtracted spectrum is dominated by GMR strength since no other multipoles has this forward peaked characteristic. The apparent flat and featureless shape at higher excitation region with statistical fluctuation centered at zero counts suggested the subtraction process is clean and

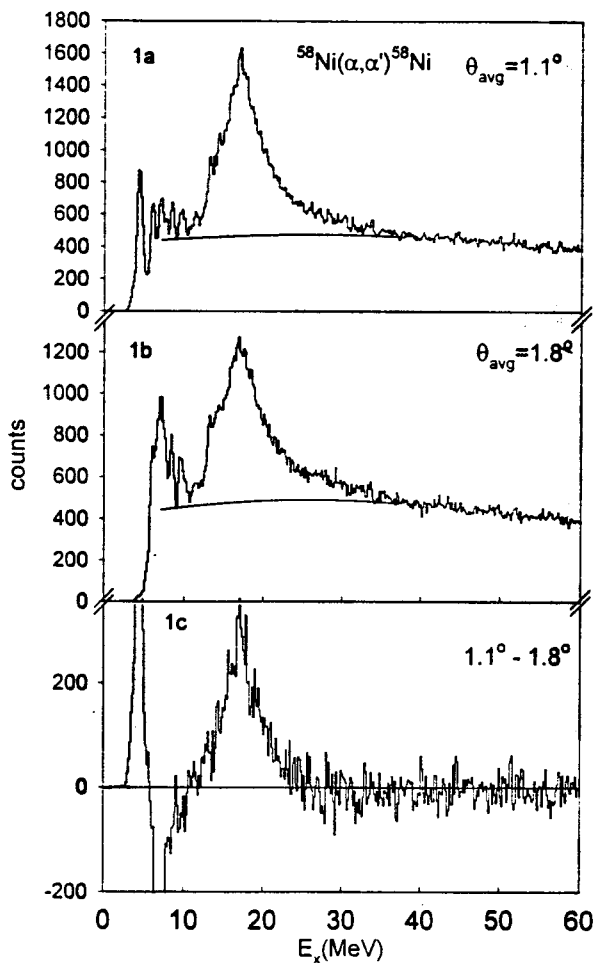


**Figure 1.** a., b. Inelastic  $\alpha$  spectra at two angles for  $^{58}\text{Ni}$ . The solid lines indicated separation between the giant resonance peak and the continuum. 1c. Difference spectrum of  $1.1^\circ - 1.8^\circ$ , the spectrum corresponding to  $\Theta_{\text{avg}}=1.8^\circ$  was subtracted from the spectrum corresponding to  $\Theta_{\text{avg}}=1.1^\circ$ .

contributions from other multipoles are small. The total E0 EWSR integrated from 12.0 MeV to 31.1 MeV is  $62 \pm 9\%$ . Calculations were also performed using the deformed potential and radial moment with fermi mass distribution on the data reported in Ref. [4] and a total of  $48 \pm 10\%$  of E0 EWSR is exhausted. This result is in reasonable agreement to the analysis of the current data.

#### Slice Analysis Method

Figs. 1a., b. reveal that giant resonance strength extends up to  $E_x \approx 35\text{MeV}$ , this same

feature was seen in  $^{40}\text{Ca}$ ,  $^{28}\text{Si}$  and  $^{24}\text{Mg}$  [1-3]. A continuum is estimated and subtracted, leaving a giant resonance peak. This peak is then divided into several intervals and cross sections obtained for each interval. The resulting angular distributions are then fit with Distorted-wave Born Approximation (DWBA) calculations corresponding to isoscalar  $L=0,1,2,3$  and 4 strength. The isovector dipole was also included in the calculation with the shape and sum rule percentage obtained from photonuclear work [6]. A sample of the angular distributions obtained for the giant resonance peak at two different excitation intervals are shown together with the fits in Fig. 2.

Elastic and inelastic scattering folding model calculations were performed using a density dependent single folding with a Woods-Saxon imaginary terms [7] and were carried out with the computer code PTOLEMY [8]. Input parameters for PTOLEMY were modified [9] to obtain a relativistic kinematically correct calculation. The shape of the real parts of the potentials and form factors for PTOLEMY were obtained using the codes SDOLFIN and DOLFIN [10]. The folding potentials and the calculations were described in detail by Satchler and Khoa [7]. The transition densities and sum rules for various multipolarities followed the expressions in Ref. [11]. Radial moments for  $^{58}\text{Ni}$  were obtained by numerical integration of the Fermi mass distribution with  $c=4.08$  fm and  $a=0.515$  fm. [7]. Folding model parameters are listed in Table I and the deformed potential parameters are in Ref. [12].

The GMR strength distribution from the slice analysis is shown in Fig. 3 and a total of  $73.6 \pm 7.7\%$  of E0 EWSR is located between 12.0 and 31.1 MeV with a centroid at  $20.30 \pm 0.24$  MeV. It

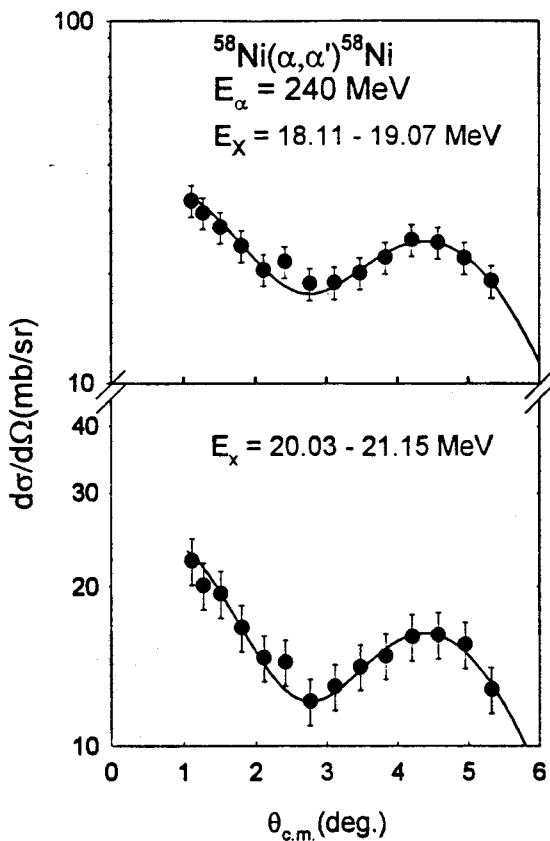


**Figure 2.** Angular distributions of the differential cross section for inelastic  $\alpha$  scattering at two excitation regions of the giant resonance peak. The solid lines are the DWBA calculations for the sum of all the distributions of the multipoles which contribute.

is in good agreement with the strength distribution obtained from the spectrum subtraction method. The result of the spectrum subtraction analysis on the earlier data is also shown in Fig. 3 together with the sum of the Gaussian peak fits from Ref. [4] and they are in reasonable agreement with the result from slice analysis of the new data.

**Table I.** Folding parameters used in the DWBA calculations.

V	W	$r_i$	$a_i$	$R_p$	$R_T$
(MeV)	(MeV)		(fm)		
41.49	40.39	0.821	0.974	1.336	1.256

$R_p$  is the coulomb radius parameter for projectile and  $R_T$  is radius parameter for target.

The centroid ( $m_1/m_0$ ) and strength of the GMR for different analysis method as well as from different data are listed in Table II. The E0 EWSR are in good agreement between different sets of data and between different analysis methods. The slice analysis shows more strength at higher excitation region than the spectrum subtraction method, it is reasonable since the data include angular distribution information therefore it is sensitive to the different shapes of the angular distributions especially for the forward peaked GMR angular distribution. On the other hand, the spectrum subtraction method relies on the uniformity of angular distribution over the entire excitation region. With other multipoles existed at higher excitation region with increasing cross-section towards larger angles, it is quite possible that subtraction process is overestimated at higher excitation region, therefore it underestimated the GMR strength. This can be seen in Fig. 1, a very slight negative counts at around 25 to 30 MeV excitation region.

The differences between the current result and the one reported earlier are two-fold. First, in Ref. [4], the sum rule strength was obtained with a square well approximation where now we are using the radial moments of the fermi mass distribution. Also in Ref. [4] the deformation parameter  $\beta$  was assumed constant ( $\beta_{\text{sum rule}} = \beta_{\text{potential}} = \beta_{\text{real}} = \beta_{\text{imaginary}}$ ) where as now the deformation lengths are assumed constant ( $\beta_{\text{mass}c} = \beta_{\text{potential}}R_{\text{potential}} = \beta_{\text{real}}R_{\text{real}} = \beta_{\text{imaginary}}R_{\text{imaginary}}$ ). Second, the continuum was overestimated in determining the giant resonance peak, thus, the strength extracted from the Gaussian peak fits are smaller. However, the effect of the continuum error is much smaller than the changes in the calculation of the sum rule and DWBA since there is not a lot of E0 strength at excitation regions

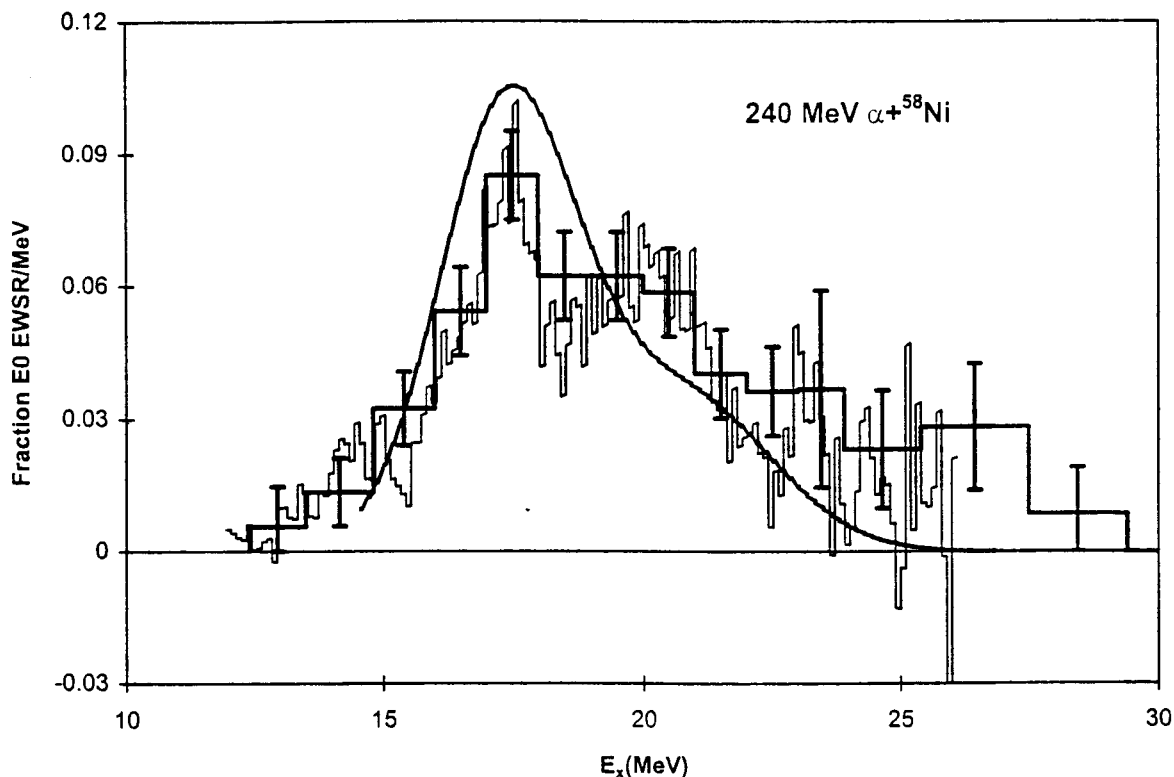


**Figure 3.** E0 strength distributions. The thick dark histogram is result from slice analysis. The dark histogram is the spectrum subtraction analysis from earlier  $^{58}\text{Ni}$  data. The solid curve line is the Gaussian peak fits from Ref. [4].

higher than 25 MeV. The current result with 74% of E0 EWSR in  $^{58}\text{Ni}$  is now more consistent with other nuclei.

**Table II.** The percentage of the E0 EWSR from different analyses and from different set of data.

Excitation region	% EWSR	Centroid ( $m_1/m_0$ ) (MeV)	analysis
12.0 < $E_x$ < 31.1 MeV	74±8	20.30±.24	slice
12.0 < $E_x$ < 31.1 MeV	62±9	18.66±0.21	subtraction
12.0 < $E_x$ < 26.5 MeV	48±10	18.71±0.25	subtraction*

\*analysis was done on the  $^{58}\text{Ni}$  data reported in Ref. [4].

## References

- [1] D.H. Youngblood, Y.-W. Lui and H.L. Clark, Phys. Rev. C **55**, 2811 (1997).
- [2] D.H. Youngblood, H. L. Clark and Y.-W. Lui, Phys. Rev. C **57**, 1134 (1998).
- [3] D.H. Youngblood, Y.-W. Lui and H.L. Clark, Phys. Rev. C (in press).
- [4] D.H. Youngblood, H.L. Clark and Y.-W. Lui, Phys. Rev. Lett **76**, 1429 (1996).
- [5] D.H. Youngblood, H.L. Clark and Y.-W. lui, Phys. Rev. Lett. **82**, 691 (1999).
- [6] S.S. Dietrich and B.L. Berman, Atomic and Nucl. Data Tables **38**, 199 (1988).

- [7] G.R. Satchler and Dao T. Khoa, Phys. Rev. C **55**, 285 (1997).
- [8] M. Rhoades-Brown, M.H. Macfarlane and S.C. Pieper, Phys. Rev. C **21**, 2417 (1980); M.H. Macfarlane and S.C. Pieper, Argonne National Laboratory Report No. ANL-76-11, Rev. 1, 1978 (unpublished).
- [9] G.R. Satchler, Nucl. Phys. **A540**, 533 (1992).
- [10] L.D. Rickerston, The folding program DOLFIN, 1976 (unpublished).
- [11] G.R. Satchler, Nucl. Phys. **A472**, 215 (1987).
- [12] H.L. Clark, Y.-W. Lui and D.H. Youngblood, Nucl. Phys. **A589**, 416 (1995).